

Temperature dependence of the electron spin g factor in CdTe and InP

Pawel Pfeffer* and Wlodek Zawadzki
Institute of Physics, Polish Academy of Sciences
Al.Lotnikow 32/46, 02-668 Warsaw, Poland

(Dated: June 10, 2022)

Temperature dependence of the electron spin g factors in bulk CdTe and InP are calculated and compared with experiment. It is assumed that the only modification of the band structure related to temperature is a dilatation change in the fundamental energy gap. The dilatation changes of fundamental gaps are calculated for both materials using available experimental data. Computations of the band structures in the presence of a magnetic field are carried out employing five-level $\mathbf{P}\cdot\mathbf{p}$ model appropriate for medium-gap semiconductors. In particular, the model takes into account spin splitting due to bulk inversion asymmetry (BIA) of the materials. The resulting theoretical effective masses and g factors increase with electron energy due to band nonparabolicity. Average g values are calculated summing over populated Landau and spin levels properly accounting for the thermal distribution of electrons in the band. It is shown that the spin splitting due to BIA in the presence of magnetic field gives observable contributions to g values. Our calculations are in good agreement with experiment in the temperature range of 0 K to 300 K for CdTe and 0 K to 180 K for InP. The temperature dependence of g is stronger in CdTe than in InP due to different signs of the band-edge g values in the two materials. Good agreement between the theory and experiment strongly indicates that the temperature dependence of spin g factors is correctly explained. In addition, we discuss formulas for the energy dependence of spin g factor due to band nonparabolicity, which are liable to misinterpretation.

PACS numbers: 72.25.Fe, 71.70.Ej, 72.25.Rb, 78.47.-p

I. INTRODUCTION

Temperature dependence of the bulk electron spin g factor in semiconductors is of interest both for scientific reasons as well as for possible spintronic applications. As far as the theory is concerned, a correct description of electron spin properties can test validity of the $\mathbf{k}\cdot\mathbf{p}$ theory for nonzero temperatures. As to the experiment, it is now possible to measure the electron spin g value up to the room temperature using quantum beats in a time-resolved photoluminescence of spin states and related effects. The latter furnished a consistent experimental picture of $g(T)$ for electrons in GaAs (see Ref. 1 and the references therein). It was shown that one can successfully describe the g factor if, in the nonparabolic $\mathbf{k}\cdot\mathbf{p}$ theory, one takes the dilatation change of the energy gap, in agreement with previous theoretical predictions²⁻⁴. On the other hand, one should account for the obvious fact that, as the temperature increases, more and more Landau and spin levels are populated by electrons. In nonparabolic conduction bands of III-V compounds the g factors change with electron energy from their values at the band edge to the free electron value +2 at high energies^{5,6}. Since g depend on electron energy, one measures in reality their values averaged over all populated levels.

In our present paper we are concerned with temperature dependences of the bulk electron g factors in CdTe

and InP. The temperature variations of g in these materials have been measured but the theoretical descriptions are missing^{7,8}. Ito et al⁸ attributed almost all the temperature variation of g in CdTe to the far-band contributions which was clearly not justified, as the authors themselves recognized. Thus, the subject can be regarded as controversial, as was previously the case for GaAs, see Refs. 7, 9, 10.

The band structure of CdTe and InP is similar to that of GaAs. In CdTe the g value is negative at the band edge and it tends to +2 going through zero as the energy increases. In InP the g value is positive at the band edge so that, tending to +2, its energy dependence is much slower. Thus we deal with two distinctly different cases. Another aspect of the present work is the spin splitting due to the bulk inversion asymmetry (BIA), called the Dresselhaus splitting¹¹. This splitting leads to a number of effects, also in the presence of an external magnetic field. In our description we account for the spin splitting due to BIA at finite magnetic fields and discuss this contribution. To our knowledge, this problem has not been considered before.

Our work has three objectives. First, we describe the temperature dependence of the electron g factors in CdTe and InP and compare the theory with existing experimental data. Second, we analyze the temperature dependences of g values in the two cases and show that they result from the opposite signs of g at the band edges of both materials. Third, we study the effect of Dresselhaus spin splitting at finite magnetic fields on the g value. Finally, we discuss validity of a frequently employed formula for the energy dependence of g factor in

* e-mail address: pfeff@ifpan.edu.pl

III-V and II-VI compounds and indicate how it should be used. Our paper is organized in the following way. In Section II we summarize the band structure calculations and indicate how the average g values are computed. In Section III we describe our calculations for CdTe and compare them with experimental data, Section IV contains similar program for InP. In Section V we discuss our results and in Section VI we summarize them. In Appendix we consider the energy dependence of g value, liable to misinterpretation.

II. THEORY

InP and CdTe are medium-gap semiconductors (MGS) and a three-level $\mathbf{k}\cdot\mathbf{p}$ description, successfully used for narrow gap semiconductors^{12,13}, is not adequate for describing their band structures. The reason is that in MGS the fundamental gap E_0 between the Γ_6^c and Γ_8^v levels is not much smaller than the gap E_1 between the Γ_6^c level and the upper Γ_7^c conduction level. It has been demonstrated that an adequate way to treat the conduction band of MGS is to use a five-level model (5LM), which is equivalent to 14 bands (including spin) in the $\mathbf{k}\cdot\mathbf{p}$ description (see Refs. 14, 15 and the references therein). According to the five-level model the spin g value at the conduction band edge is [14],

$$g_0^* = 2 + \frac{2}{3} \left[E_{P_0} \left(\frac{1}{E_0} - \frac{1}{G_0} \right) + E_{P_1} \left(\frac{1}{G_1} - \frac{1}{E_1} \right) \right] + \frac{4\overline{\Delta}\sqrt{E_{P_0}E_{P_1}}}{9} \left(\frac{2}{E_1G_0} + \frac{1}{E_0G_1} \right) + 2C' , \quad (1)$$

where $E_{P_0} = 2m_0P_0^2/\hbar^2$, $E_{P_1} = 2m_0P_1^2/\hbar^2$, $G_0 = E_0 + \Delta_0$ and $G_1 = E_1 + \Delta_1$. The spin-orbit energies Δ_0 and Δ_1 relate to (Γ_7^v, Γ_8^v) and (Γ_7^c, Γ_8^c) levels, respectively, $\overline{\Delta}$ is the interband matrix element of the spin orbit interaction between the (Γ_7^v, Γ_8^v) and (Γ_7^c, Γ_8^c) multiplets (see [14, 16]), and C' is due to far-band contributions. Figure 1 shows schematically the five-level $\mathbf{k}\cdot\mathbf{p}$ model used in our calculations. For $\overline{\Delta} = 0$ Eq. (1) reduces to the formula given first by Hermann and Weisbuch¹⁷. Calculating the electron energies away from the band edge one deals with the effects of band's nonparabolicity and inversion asymmetry. In particular, an appearance of the matrix element Q is due to the bulk inversion asymmetry. Since the 5LM for electrons in the presence of a magnetic field and its use for magneto-optical properties of MGS was described in some details before^{14,15}, we only mention here the main elements of this approach. Thus the model includes exactly the $\Gamma_7^v, \Gamma_8^v, \Gamma_6^c, \Gamma_7^c$ and Γ_8^c levels at the center of the Brillouin zone and the resulting $\mathbf{k}\cdot\mathbf{p}$ matrix has dimensions 14×14 . There exist three nonvanishing interband matrix elements of momentum: P_0, P_1 and Q . If one takes $Q = 0$ and $k_z = 0$ (where $\hbar k_z$ is the momentum along the magnetic field) the 14×14 initial matrix factorizes into two 7×7 matrices for the

spin-up and spin-down states. These matrices are soluble by envelope functions in the form of harmonic oscillator functions and the eigenenergy problem for different Landau levels (LLs) n reduces to diagonalization of 7×7 determinants.

Taking the asymmetric gauge for the vector potential $\mathbf{A} = [-By, 0, 0]$ one obtains the harmonic oscillator functions in the form $\exp(ik_x x + ik_z z)\Phi_n[(y - y_0)/L]$, where $y_0 = k_x L^2$. Here $L = (\hbar/eB)^{1/2}$ is the magnetic radius. If the Q element is included (it comes from an inversion asymmetry of MGS crystals) the initial 14×14 matrix does not factorize and is not soluble in terms of a single column of harmonic oscillator functions. Physically, this means that the resulting energy bands are not spherical. Since the nonsphericity of the conduction bands in MGS is small, one can find the eigenenergies looking for the envelope functions in terms of sums of harmonic oscillator functions (see Ref. 18). This leads to number determinants composed of the fundamental 7×7 blocks on the diagonal coupled by nondiagonal parts involving Q and k_z elements. The eigenenergies are computed truncating the resulting big determinants. In our computations we used typically 112×112 determinants. All calculations were performed taking a magnetic field \mathbf{B} parallel to the [001] direction.

Next, we consider average values of the spin g factor measured as a function of temperature. The measurements are usually done in relatively pure samples having low free electron densities. The electrons are excited across the gap into the conduction band and into both spin states. The spin states are almost equally populated and the circularly polarized light produces a well defined coherence between them. The excited electrons quickly thermalize and are distributed among Landau levels (LLs) according to the lattice temperature without losing their spin or phase. Then they interfere and quantum beats in the photoluminescence or other effects are observed from many LLs. According to this picture the observed signal represents an average over the populated levels. The electron thermal distribution over LLs determines their contribution to the average g value.

We assume the k_z -dependence of electron energies in a simplified form

$$\mathcal{E}_{nk_z}^\pm = \mathcal{E}_n^\pm + \frac{\hbar^2 k_z^2}{2m_0^*} , \quad (2)$$

where n is the LL number, \pm signs correspond to the two spin states, k_z is the wavevector along the direction of \mathbf{B} , and m_0^* is the effective mass at the band edge. The description of energies \mathcal{E}_n^\pm contains the intricacies of the band structure mentioned above. The spin g value is defined as (in formulas we use g^* symbol)

$$g^* = (\mathcal{E}_{nk_z}^+ - \mathcal{E}_{nk_z}^-)/\mu_B B. \quad (3)$$

An averaging procedure involves a summation over n and integrations over k_x and k_z . A simple calculation gives the average value of g^* in the form

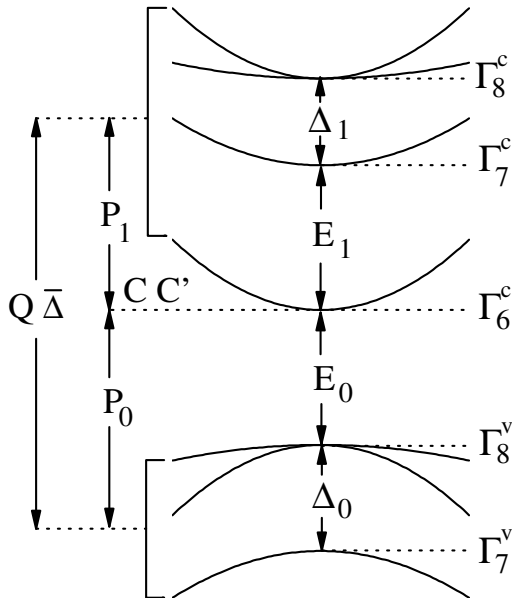


FIG. 1: Five-level $\mathbf{P}\cdot\mathbf{p}$ model of band structure in medium-gap semiconductors CdTe and InP. The zero of energy is chosen at the Γ_6^c edge. Interband matrix elements of momentum P_0 , P_1 , Q as well as interband matrix element of spin-orbit interaction $\bar{\Delta}$ are indicated, C and C' symbolize far-band contributions to the band-edge effective mass and spin g factor, respectively.

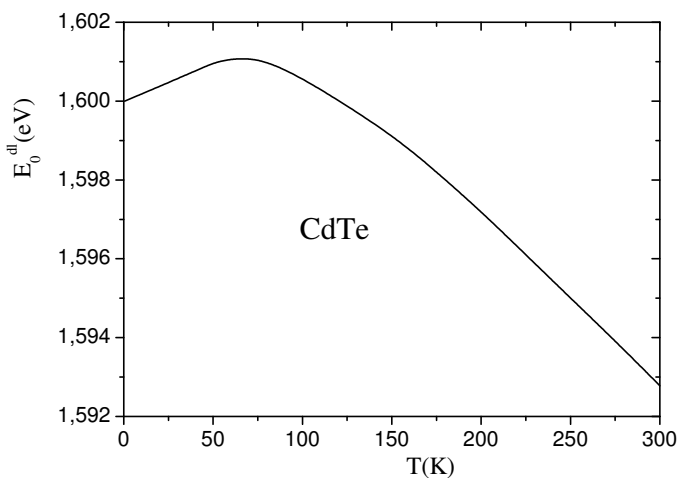


FIG. 2: Dilatation gap $E_0(T)$ in CdTe versus temperature calculated from Eq.(7) with the use of experimental values of D , $\partial E_0/\partial P$ and $\alpha_{th}(T)$, see Eq. (2).

$$\bar{g}^*(T) = \frac{A}{C}, \quad (4)$$

where

$$A = \sum_{n=0}^{\infty} \int_{\mathcal{E}_n^i}^{\infty} \frac{g_n^*(\mathcal{E})f(\mathcal{E}, \zeta)}{(\mathcal{E} - \mathcal{E}_n^i)^{1/2}} d\mathcal{E}, \quad (5)$$

and

$$C = \sum_{n=0}^{\infty} \int_{\mathcal{E}_n^i}^{\infty} \frac{f(\mathcal{E}, \zeta)}{(\mathcal{E} - \mathcal{E}_n^i)^{1/2}} d\mathcal{E}, \quad (6)$$

in which the summation is over the LLs, $f(\mathcal{E}, \zeta)$ is the Fermi-Dirac distribution function, and the square roots come from the integrations over k_z . The integrations begin from the lower of the two states \mathcal{E}_n^i for each n , which can be either \mathcal{E}_n^+ or \mathcal{E}_n^- depending on the sign of the g value.

The average g value, as given by Eq. (4), is affected by the temperature in two opposite ways. As the temperature T increases and the absolute value of the fundamental gap E_0 decreases, the spin g_0^* value at the band edge decreases. On the other hand, with increasing T the electrons populate higher LLs and band's nonparabolicity comes more and more into play. The latter is known to make the g value less negative (see Refs. 5, 6). Thus, as T increases, the average g^* decreases or increases depending on the relative strength of the two effects. We emphasize that we do not use in our calculations Eq. (1), it is quoted only to make clear the dependence of g_0^* on E_0 and other parameters.

III. CdTe

As mentioned above, it was demonstrated that the temperature change in the effective mass and the spin g factor in a material is governed by a *dilatational* variation of energy gaps, of which the fundamental gap is of primary importance. Thus one needs to determine the dilatational change in the fundamental gap due to temperature since the directly measured total temperature change is due to both the dilatation of the crystal lattice and its vibrations (phonons). We quote the determination of $E_0^{dl}(T)$ for CdTe since, to our knowledge, it has not been carried out before. The dilatational change in the gap is given by

$$\Delta E_0^{dl}(T) = -3D \left(\frac{\partial E_0}{\partial P} \right)_T \int_0^T \alpha_{th}(T') dT', \quad (7)$$

where D is the bulk modulus, $\partial E_0/\partial P$ is the pressure-induced gap shift, and $\alpha_{th}(T)$ is the linear thermal expansion coefficient (see also Ref. 19). The quantities D and $\partial E_0/\partial P$ are directly measurable, for CdTe there is

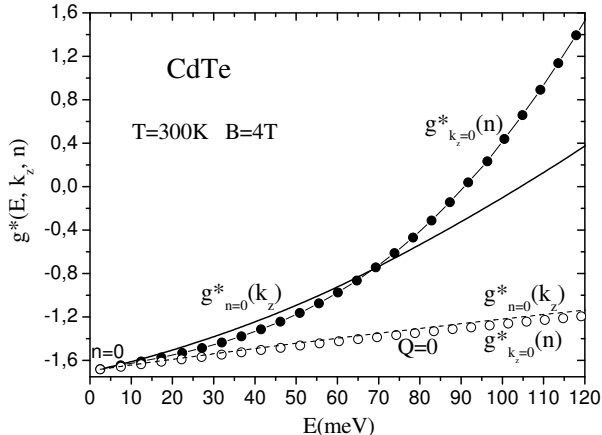


FIG. 3: Calculated spin g factor in bulk CdTe versus electron energy in the conduction band. Full points are g values for consecutive LLs and $k_z = 0$, solid line indicates g value for $n = 0$ as a function of k_z , empty points and dashed line: the same as above but neglecting bulk inversion asymmetry (i.e. putting $Q = 0$).

$\partial E_0/\partial P = 0.08$ eV/GPa^{20,21} (see also Refs. 22-26) and $D = 42$ GPa²⁶. The linear thermal expansion coefficient $\alpha_{th}(T)$ was calculated²⁸ and measured²⁹. Using these results we performed the integration indicated in Eq. (7) and obtained the dilatational variation of the fundamental gap in CdTe shown in Fig. 2. It is seen that $E_0^{dl}(T)$ goes through a maximum at $T \approx 65$ K but, all in all, the temperature variation between 0 K and 300 K is rather small.

Knowing $E_0^{dl}(T)$ and assuming that other gaps, momentum matrix elements and far-bands contributions do not depend on the temperature, one can perform the band structure calculations outlined above if the band parameters are known. For CdTe we take the following parameter values at $T = 0$: $E_{P_0} = 21.07$ eV, $E_{P_1} = 5.1$ eV, $E_Q = 13.29$ eV (see Ref. 30), $E_0 = -1.6$ eV³¹, $\Delta_0 = -0.95$ eV^{32,33}, $E_1 = 3.76$ eV^{34,35}, $\Delta_1 = 0.27$ eV³⁰, $\bar{\Delta} = -0.19$ eV³⁰, $C = -0.5355$ and $C' = -0.0129$. The far-band contributions are taken to obtain at $T = 0$ the band edge values $m_0^* = 0.093 m_0$ ³⁶ and $g_0^* = -1.66$ ⁹. The zero of energy is chosen at the Γ_6^c edge, see Fig. 1, so the energies above are positive while the energies below are negative.

Figure 3 shows the result of our intermediate calculations for CdTe, given as example. The calculations are performed for fixed values of T and B . In order to investigate the effect of BIA on the g value at finite B we carried out the computations in two versions: 1) using the full 5LM, i. e. including the matrix element Q which, as mentioned above, incorporates BIA (full points and solid line); 2) putting $Q = 0$, i. e. neglecting the effect of BIA (empty points and dashed line). The full points in Fig. 3 indicate calculated spin g values for consecutive LLs (at $k_z = 0$) beginning with LL $n = 0$. It is seen that the g value increases with the LL number n (or, equivalently,

the energy) due to band's nonparabolicity. The solid line shows the calculated g for $n = 0$ as a function of k_z (or, equivalently, the energy). It can be seen that, for lower LL numbers n , the g value behaves very similarly for n -dependence and k_z -dependence. As argued by the present authors³⁷, the above dependences should be identical within the description by the three-level model, see also Appendix. The empty points and dashed line show the corresponding quantities calculated with $Q = 0$. Here both $g^*(n, k_z = 0)$ and $g^*(n = 0, k_z)$ are practically the same. The differences between the full points (and solid line) and the empty points (and dashed line) are directly due to the effect of BIA.

It is well known that, in the absence of magnetic field, the spin splitting due to BIA is $\Delta\mathcal{E} = 2\gamma[k^2(k_x^2k_y^2 + k_x^2k_z^2 + k_y^2k_z^2) - 9k_x^2k_y^2k_z^2]^{1/2}$. For the presence of B we can not give an analytical expression for the spin splitting due to BIA. However, one can qualitatively say that, at $B \neq 0$, k_x and k_y components are replaced by $(nB)^{1/2}$ or $[(n+1)B]^{1/2}$ terms, while the k_z component along the magnetic field remains the same. For $n = 0$ the "transverse" components are small (or zero) and for $\mathcal{E} \approx 0$ the longitudinal component $k_z \approx 0$, so that BIA gives almost no contribution, which agrees with the results shown in Fig. 3. The increasing energy \mathcal{E} corresponds to the increase of n or k_z (or both), so the contribution of BIA grows. This is reflected by an increasing difference of the results for $Q \neq 0$ and $Q = 0$ shown in Fig. 3.

We follow the similarity of $g^*(n = \text{const}, k_z)$ and $g^*(n, k_z = \text{const})$ dependences shown in Fig. 3 assuming $g^*(n = \text{const}, k_z)$ to be equal to $g^*(n, k_z = \text{const})$ in the summation of LLs and integration over k_z , see Eqs. (5) and (6). This approximation is in fact quite good since the region of high energies: $\mathcal{E} \geq 90$ meV for CdTe (see Fig. 3), where this approximation begins to break down, is weakly populated by electrons and it gives only small contribution to the average g value.

Using the above assumption we performed the summation and integration indicated in Eqs. (5) and (6) and determined the average value of g according to Eq. (4). Our final results for CdTe are shown in Fig. 4. It can be seen that the experimental values of Oestreich et al⁷ (lower temperatures) and that of Ito et al⁸ (room temperature) are described very well. For temperatures above 200 K the theory is slightly higher than experiment. We conclude that the main reason behind the observed increase of the spin g value with temperature is that, as the temperature increases, higher Landau and spin levels contribute to the average g value. Since the band structure predicts an increase of g with growing energy (see also the discussion in Appendix) the resulting average g becomes higher (less negative). This mechanism is well illustrated in the inset of Fig. 4.

IV. InP

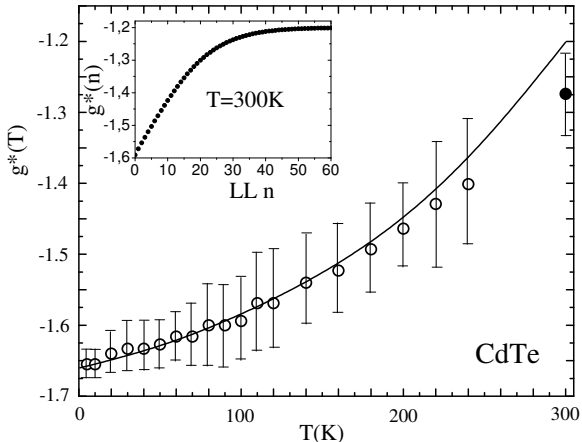


FIG. 4: Spin g factor in bulk CdTe versus temperature. Empty points: experimental data of Ref. 7, full point: data of Ref. 8. Solid line: theoretical average g factor calculated according to Eq. (4). Inset shows how consecutive LLs contribute to the average g value at $T = 300$ K.

InP is a medium-gap semiconductor similar in many respects to GaAs. However, the electron spin g factor at the band edge of InP is positive, in contrast to InSb, InAs, GaSb and GaAs¹⁷. Since, as we mentioned above, at high electron energies g tends to +2 (if one neglects the effects of BIA) there remains not much room for the energy variation of g value.

The dilatational change in the fundamental energy gap of InP was estimated by Hazama et al⁴. However, we revise this estimation because a part of the procedure adopted in Ref. 4 was based on calculations, while in our approach we use exclusively experimental information. To determine the dilatation gap of InP we use again formula (7). We take $D = 71$ GPa^{38,39}, and $dE_0/dP = 0.084$ eV/GPa⁴⁰. As to the function $\alpha_{th}(T)$, it was measured by various authors, see Refs. 41-43. We follow the measurements of Haruna et al⁴¹, which basically agree with those of other authors but are more complete. In the data of Ref. 41 we correct the point at $T = 8$ K (since the given value $\alpha_{th}(8K)$ has the wrong sign) by interpolating between the measured values at 0 K and 15 K. The complete function $\alpha_{th}(T)$ is then used for the numerical integration indicated in Eq. (7). Our final results for $E_0^{dl}(T)$ are shown in Fig. 5; the obtained variation in the dilatation gap is noticeably smaller than that given in Ref. 4. We use the results indicated in Fig. 5 in our further procedure.

To perform the band structure calculations we take the following band parameters⁴⁴: $E_{P_0} = 20.93$ eV, $E_{P_1} = 0.165$ eV, $E_Q = 15.56$ eV, $E_0 = -1.423$ eV, $\Delta_0 = -0.108$ eV, $E_1 = 3.297$ eV, $\Delta_1 = 0.201$ eV, $\overline{\Delta} = 0.08733$ eV⁴⁵, $C = -2.467$ and $C' = -0.08045$. The far-band contributions are taken to obtain at $T = 0$ the band edge values $m_0^* = 0.07927m_0$ ³⁶ and $g_0^* = +1.204$. Our band structure calculations are performed similarly to those described

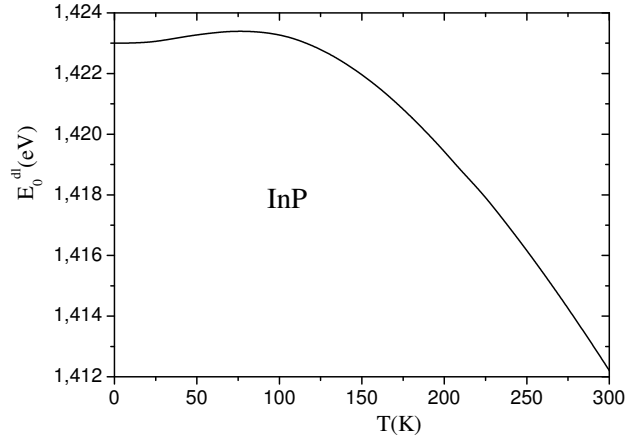


FIG. 5: The same as in Fig. 2 but for InP.

above for CdTe.

In Fig. 6 we show intermediate calculated results for $g^*(n, k_z = 0)$ and $g^*(n = 0, k_z)$ according to the 5LM in two versions: 1) including the matrix element Q , i.e. including BIA (full points and solid line); 2) putting $Q = 0$, i.e. neglecting BIA (empty points and dashed line). Again, as discussed above, in the region of energies $\mathcal{E} \leq 190$ meV the two dependences are very similar (for $Q = 0$ they practically coincide for all energies) so that, when performing the integration over k_z in Eq. (5) we assume that the k_z -dependence of g value for each LL is the same as that given by the black points. As far as the contribution of BIA to the spin splitting is concerned, the picture is similar to that for CdTe: at low energies the contribution of BIA vanishes but it grows with the energy. Clearly, in our final calculations we do take into account the effect of BIA.

Figure 7 shows our final results for the temperature dependence of the average g value in InP, computed according to Eqs.(4)-(6). It is seen that the available experimental data of Oestreich et al [7] are described very well. Similarly to CdTe, the main reason for the increase of g value with the temperature is that, as T grows, more Landau and spin levels in the nonparabolic conduction band of InP are populated with electrons. On the other hand, the temperature variation of average g in InP is considerably weaker than that in CdTe for reasons given above.

V. DISCUSSION

One should bear in mind that the g values measured by various authors do not agree too well with each other. For CdTe, Meyer et al⁴⁶ used the spin resonance to measure g values in the temperature range of $4.2 \text{ K} \leq T \leq 66$ K and obtained the data which can be described by the linear dependence $g^*(T) = -1.682 + 2.97 \times 10^{-4} T$. All these values are somewhat lower than those shown in

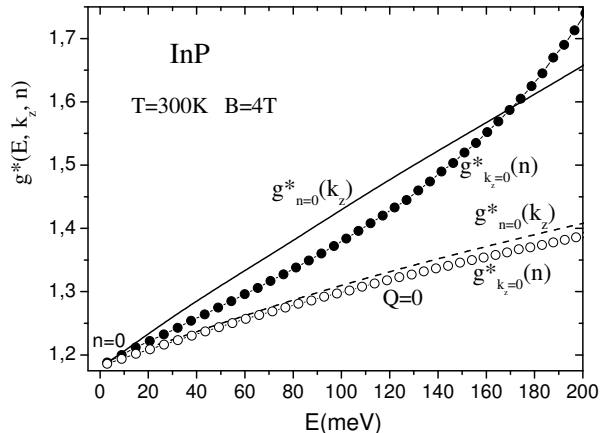


FIG. 6: The same as in Fig. 3 but for InP.

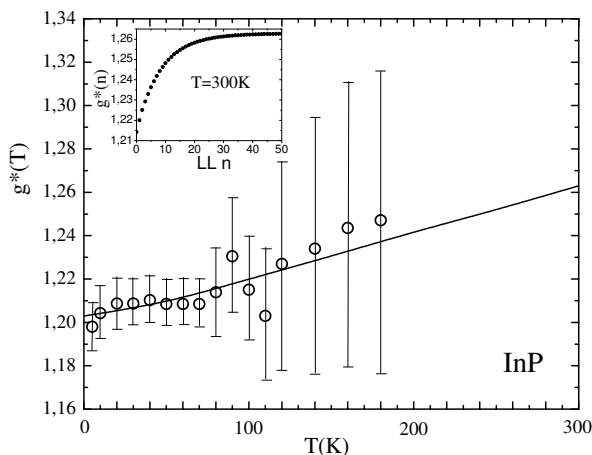


FIG. 7: Spin g factor in bulk InP versus temperature. Empty points: experimental data of Ref. 7. Solid line: theoretical average g factor calculated according to Eq. (4). Inset shows how consecutive LLs contribute to the average g value at $T = 300$ K.

Fig. 4. Sprinzl et al⁴⁷ used the spin quantum beats to measure the g values that agree with those shown in Fig. 4 at low temperatures but are considerably lower near room temperature. We believe that the data shown in Fig. 4 are reliable since the lower temperature results of Oestreich et al⁷ are consistent with the result of Ito et al⁸ for $T = 300$ K.

As for InP, we note that the low-temperature result of Weisbuch and Hermann⁴⁸ $g_0^* = +1.26$, obtained with the use of spin resonance, is distinctly higher than the values shown in Fig. 7. However, such differences between measured g values are not unusual, see Fig. 4 of Ref. 1 for GaAs. We were unable to find experimental measurements of the g factor in InP for temperatures above 200 K.

As follows from Figs. 3 and 6, the g values calculated taking $Q \neq 0$, i.e. using the complete 5LM description,

are for higher electron energies considerably higher than those obtained taking $Q = 0$. This means that the agreements between experiment and theory shown in Figs. 4 and 7 give clear indications that the influence of bulk inversion asymmetry on the spin splitting at $B \neq 0$ is not negligible in CdTe and InP. This evidence is still somewhat indirect since the average values are given by sums over many LLs and integrations over k_z . However, as each term of the sum over LLs and the integration over k_z is affected by BIA, the evidence for its non-negligible effect seems convincing. One could verify more directly the effect of BIA in the presence of a magnetic field by investigating at low temperatures an anisotropy of the spin splitting with respect to the orientation of a magnetic field. It should be mentioned that the effect of BIA on the g values of heavy holes in GaAs quantum wells was recently investigated by Kubisa et al⁴⁹.

Finally, we believe that the distinctly different temperature dependences of spin g values in CdTe and InP, both experimental and theoretical, are significant. The increase of g in CdTe between $T \approx 0$ and $T = 180$ K is $\Delta g^* \approx 0.16$, while in InP the increase in the same temperature range is $\Delta g^* \approx 0.049$. As we remarked above, this difference is due to different energy dependences of g factors in the two materials because at high energies the g factor should reach the free-electron value of +2 (if one neglects BIA), while the initial band-edge value in CdTe is $g_0^* \approx -1.66$ and in InP it is $g_0^* \approx +1.20$. In consequence, $g^*(\mathcal{E})$ dependence in InP is distinctly weaker than that in CdTe. The above reasoning is confirmed experimentally which strongly indicates that our interpretation, as described above, is correct. We emphasize this conclusion since the reason for the temperature dependence of the spin g factor remains to be a matter of controversy, cf. Ref. 10.

VI. SUMMARY

Dilatational changes in the fundamental energy gaps of CdTe and InP are determined from available experimental data in order to use them in calculations of band structures at nonzero temperatures. The five-level $\mathbf{P}\text{-}\mathbf{p}$ model is employed to compute the band structures of these medium-gap semiconductors in the presence of a magnetic field. In particular, energy dependences of the electronic spin g factors due to band nonparabolicities are obtained. Next, average g values are calculated for different temperatures summing over populated Landau and spin levels and integrating over longitudinal momentum $\hbar k_z$. The increase of g 's with growing temperature are almost exclusively due to the population of higher Landau and spin levels in nonparabolic conduction bands. The calculated $g^*(T)$ dependences are compared with available experimental values and good agreement between experiment and theory is obtained for both materials. The temperature increase of spin g factor is stronger in CdTe than in InP, which is related to the negative band-

edge value of g in CdTe and the positive one in InP. It is shown that the bulk inversion asymmetry gives observable contributions to the spin splittings in the presence of a magnetic field. Frequently used formulas for the energy-dependent spin g factors in nonparabolic conduction bands of III-V compounds are discussed.

Appendix

Since our work is closely related to dependence of the electron spin g factor on the electron energy \mathcal{E} in III-V and some II-VI semiconductor compounds, we discuss here the use of an often employed formula for $g^*(\mathcal{E})$. To the best of our knowledge, the first description of $g^*(\mathcal{E})$ in narrow-gap III-V compounds was given in 1961 by Lax, Mavroides, Zeiger, and Keyes⁵ (LMZK) and a different but equivalent formula was derived in 1963 by Zawadzki⁶. The formula of LMZK, although old, is still used in the literature (see for example Refs. 8, 50-52) so it merits a discussion.

It is important to see how the formula is derived. The underlying formulation is due to Bowers and Yafet¹², see also Ref. 6. The three-level $\mathbf{P}\cdot\mathbf{p}$ description (see Refs. 12, 53) takes into account the Γ_6^c conduction level and Γ_8^v , Γ_7^v valence levels. The resulting $\mathbf{P}\cdot\mathbf{p}$ 8×8 Hamiltonian is solved in terms of harmonic oscillator functions neglecting small free-electron terms. Final equation for the energies is obtained in the form

$$\mathcal{E}(\mathcal{E} - E_0)(\mathcal{E} - E_0 - \Delta_0) + P_0^2[s(2n+1) + k_z^2](\mathcal{E} - E_0 - \frac{2}{3}\Delta_0) \mp \frac{1}{3}P_0^2\Delta_0 s = 0, \quad (\text{A.1})$$

where $s = eB/\hbar$ and other symbols have been defined above. For specified B, n, k_z and the spin sign \pm , Eq. (A.1) represents a cubic equation for the energy $\mathcal{E}(n, k_z, \pm)$. In order to proceed further, we divide Eq. (A.1) by $(\mathcal{E} - E_0)(\mathcal{E} - E_0 - \Delta_0)$ and after a simple algebraic manipulation obtain for the conduction band

$$\mathcal{E}_{nk_z}^\pm = \frac{\hbar e B}{m^*(\mathcal{E}_{nk_z}^\pm)}(n + \frac{1}{2}) + \frac{\hbar^2 k_z^2}{2m^*(\mathcal{E}_{nk_z}^\pm)} \pm \frac{\mu_B B}{2} g^*(\mathcal{E}_{nk_z}^\pm) \quad (\text{A.2})$$

where

$$\frac{m_0}{m^*(\mathcal{E}_{nk_z}^\pm)} = 1 - \frac{E_{P_0}}{3} \left(\frac{2}{\tilde{E}_0^\pm} + \frac{1}{\tilde{G}_0^\pm} \right); \quad (\text{A.3})$$

$$g^*(\mathcal{E}_{nk_z}^\pm) = 2 + \frac{2E_{P_0}}{3} \left(\frac{1}{\tilde{E}_0^\pm} - \frac{1}{\tilde{G}_0^\pm} \right) \quad (\text{A.4})$$

in which

$$\tilde{E}_0^\pm = E_0 - \mathcal{E}_{nk_z}^\pm, \quad (\text{A.5})$$

$$\tilde{G}_0^\pm = E_0 + \Delta_0 - \mathcal{E}_{nk_z}^\pm. \quad (\text{A.6})$$

The additive terms $+1$ in Eq. (A.3) and $+2$ in Eq. (A.4) result from the free-electron contributions in the $\mathbf{P}\cdot\mathbf{p}$ theory, which were neglected in the original Bowers and Yafet treatment¹², cf. Ref. 14. Equations (A.2), (A.3), (A.4) amount to the LMZK formulas in which band's nonparabolicity enters via the energy dependence of m^* and g^* (LMZK formulas do not contain the free electron terms).

The problem with the above formulation is that the energy $\mathcal{E}_{nk_z}^\pm$ on the LHS of Eq. (A.2) is the same as that entering $m^*(\mathcal{E}_{nk_z}^\pm)$ and $g^*(\mathcal{E}_{nk_z}^\pm)$ on the RHS. Suppose one fixes B, n and k_z and tries to calculate the spin splitting. It is clear that it is not enough to take the energy difference for the plus and minus signs in Eq. (A.2) and calculate the energy on LHS because both the mass $m^*(\mathcal{E}_{nk_z}^\pm)$ and the spin factor $g^*(\mathcal{E}_{nk_z}^\pm)$ have different values for different signs of the spin. In particular, if n or k_z are large, the orbital term in Eq. (A.2) is considerably different for the opposite spins which should be necessarily taken into account. In fact, the form given by LMZK and used in the literature is inconvenient since the energy $\mathcal{E}_{nk_z}^\pm$ should be determined self-consistently. It is considerably simpler to use directly Eq. (A.1) and solve for the energies. However, in most applications one simply employs formula (A.4) for the energy dependence of $g^*(\mathcal{E})$ forgetting the orbital term and the fact that in a nonparabolic band $g^*(\mathcal{E}_{nk_z}^\pm)$ is different for each spin direction.

Finally, we note that a formulation analogous to that given by LMZK for 3LM has been derived by the present authors for GaAs-type medium gap semiconductors with the use of 5LM, see Refs. 37, 54. The result is that Eq. (A.2) is still valid but the formulas for $m^*(\mathcal{E}_{nk_z}^\pm)$ and $g^*(\mathcal{E}_{nk_z}^\pm)$ become

$$\frac{m_0}{m^*(\mathcal{E}_{nk_z}^\pm)} = 1 + C - \frac{1}{3} \left[E_{P_0} \left(\frac{2}{\tilde{E}_0^\pm} + \frac{1}{\tilde{G}_0^\pm} \right) + E_{P_1} \left(\frac{2}{\tilde{G}_1^\pm} + \frac{1}{\tilde{E}_1^\pm} \right) \right] + \frac{4\overline{\Delta}\sqrt{E_{P_0}E_{P_1}}}{3} \left(\frac{1}{\tilde{E}_1^\pm\tilde{G}_0^\pm} - \frac{1}{\tilde{E}_0^\pm\tilde{G}_1^\pm} \right), \quad (\text{A.7})$$

and

$$g^*(\mathcal{E}_{nk_z}^\pm) = 2 + 2C' + \frac{2}{3} \left[E_{P_0} \left(\frac{1}{\tilde{E}_0^\pm} - \frac{1}{\tilde{G}_0^\pm} \right) + E_{P_1} \left(\frac{1}{\tilde{G}_1^\pm} - \frac{1}{\tilde{E}_1^\pm} \right) \right] - \frac{4\overline{\Delta}\sqrt{E_{P_0}E_{P_1}}}{9} \left(\frac{2}{\tilde{E}_1^\pm\tilde{G}_0^\pm} + \frac{1}{\tilde{E}_0^\pm\tilde{G}_1^\pm} \right), \quad (\text{A.8})$$

where \tilde{E}_0^\pm and \tilde{G}_0^\pm are still given by Eqs. (A.5) and (A.6), respectively, and

$$\tilde{E}_1^\pm = E_1 - \mathcal{E}_{nk_z}^\pm, \quad (\text{A.9})$$

$$\tilde{G}_1^\pm = E_1 + \Delta_1 - \mathcal{E}_{nk_z}^\pm. \quad (\text{A.10})$$

The terms proportional to E_{P_1} are related to the inter-band $\Gamma_6^c\text{-}\Gamma_8^c$ and $\Gamma_6^c\text{-}\Gamma_7^c$ interactions, see Fig. 1. On both sides of Eq. (A.2) the energy is $\mathcal{E}_{nk_z}^\pm$ and, for given B , n , k_z and \pm , this energy should be determined in a self-

consistent way. The above formulas do not contain the element Q , i.e. they neglect the effects of bulk inversion asymmetry.

-
- [1] W. Zawadzki and P. Pfeffer, R. Bratschitsch, Z. Chen, and S. T. Cundiff, B. N. Murdin, C. R. Pidgeon, Phys. Rev. B **78**, 245203 (2008).
- [2] H. Ehrenreich, J. Phys. Chem. Solids **2**, 131 (1959).
- [3] R. A. Stradling and R. A. Wood, J. Phys. C **3**, L94 (1970).
- [4] H. Hazama, T. Sugimasa, T. Imachi, and C. Hamaguchi, J. Phys. Soc. Jpn. **55**, 1282 (1986).
- [5] B. Lax, J. G. Mavroides, H. J. Zeiger, and R. J. Keyes, Phys. Rev. **122**, 31 (1961).
- [6] W. Zawadzki, Physics Lett. **4**, 190 (1963).
- [7] M. Oestreich, S. Hallstein, A. P. Heberle, K. Eberl, E. Bauser, and W. W. Ruhle, Phys. Rev. B **53**, 7911 (1996).
- [8] T. Ito, W. Shichi, Y. Okami, M. Ichida, H. Gotoh, H. Kamada, and H. Ando, phys. stat. sol. (c) **6**, 319 (2009).
- [9] M. Oestreich and W. W. Ruhle, Phys. Rev. Lett. **74**, 2315 (1995).
- [10] J. Huebner, S. Dohrmann, D. Hagele, and M. Oestreich, Phys. Rev. B **79**, 193307 (2009).
- [11] G. Dresselhaus, Phys. Rev. **100**, 580 (1955).
- [12] R. Bowers and Y. Yafet, Phys. Rev. **115**, 1165 (1959).
- [13] C. R. Pidgeon and R. N. Brown, Phys. Rev. **146**, 575 (1966).
- [14] P. Pfeffer and W. Zawadzki, Phys. Rev. B **41**, 1561 (1990).
- [15] P. Pfeffer and W. Zawadzki, Phys. Rev. B **53**, 12813 (1996).
- [16] F.H.Pollak, C.W.Higginbotham, and M.Cardona, J. Phys. Soc. Jpn. Suppl. **21**, 20 (1966).
- [17] C. Hermann and C. Weisbuch, Phys. Rev. B **15**, 823 (1977).
- [18] V. Evtuhov, Phys. Rev. **125**, 1869 (1962).
- [19] P. Lautenschlager, M. Garriga, S. Logothetidis, and M. Cardona, Phys. Rev. B **35**, 9174 (1987).
- [20] J. R. Mei and V. Lemos, Solid State Commun. **52**, 785 (1984).
- [21] D. L. Camphausen, G. A. Nevill Connell and W. Paul, Phys. Rev. Lett. **26**, 184 (1971).
- [22] G. A. Babonas, R. A. Bendoryus, and A. Yu. Shileika, Soviet Physics Semiconductors **5**, 392 (1971).
- [23] W. Shan, S. C. Shen and H. R. Zhu, Solid State Commun. **55**, 475 (1985).
- [24] M. Prakash, M. Chandrasekhar, and H. R. Chandrasekhar, Phys. Rev. B **42**, 3586 (1990).
- [25] H. M. Cheong, J. H. Burnett and W. Paul, Solid State Commun. **77**, 565 (1991).
- [26] J. Gonzalez, F. V. Perez, E. Moya and J. C. Chervin, J. Phys. Chem. Solids **56**, 335 (1995).
- [27] K. Strossner, S. Ves, W. Dieterich, W. Gebhardt and M. Cardona, Solid State Commun. **56**, 563 (1985).
- [28] D. Bagot, R. Granger, and S. Roland, phys. stat. sol. (b) **177**, 295 (1993).
- [29] G. K. White, J. G. Collins, J. A. Birch, and T. F. Smith, J. Phys. C **13**, 1649 (1980).
- [30] W. Willatzen, M. Cardona, N. E. Christensen, Phys. Rev. B **51**, 17992 (1995).
- [31] M. Nawrocki, A. Twardowski, phys. stat. sol. (b) **97**, K61 (1997).
- [32] A. Twardowski, E. Rokita, and J. A. Gaj, Sol. State. Commun. **36**, 927 (1980).
- [33] D. Niles, H. Hochst, Phys. Rev. B **43**, 1492 (1991).
- [34] V. V. Sobolev, O. G. Maksimova, S. G. Kroitoru, phys. stat. sol. (b) **103**, 499 (1981).
- [35] K. Boujdaria and O. Zitouni, Solid State Commun. **129**, 205 (2004).
- [36] E. Molva, Le Si Dang, Phys. Rev. B **27**, 6222 (1983).
- [37] P. Pfeffer and W. Zawadzki, Phys. Rev. B **74**, 115309 (2006).
- [38] V. M. Glazov, K. Davletov, A. Ya. Nashelskii and M. M. Mamedov, Zh. Fiz. Khim. **51**, 10, 2558 (1977). In Russian.
- [39] D. N. Nichols, D. S. Rimai, and J. Sladek, Solid St. Commun. **36**, 667 (1980).
- [40] H. Muller, G. Trommer, M. Cardona and P. Vogel, Phys. Rev. B **21**, 4879 (1980).
- [41] K. Haruna, H. Maeta, K. Ohashi and T. Koike, J. Phys. C **20**, 5275 (1987).
- [42] P. Deus, H. A. Schneider, U. Voland, and K. Stiehler, phys. stat. sol. (a) **103**, 443 (1987).
- [43] N. N. Sirota and A. A. Sidorov, Dokl. Akad. Nauk SSSR **284**, 1111 (1985). In Russian.
- [44] M. A. Hopkins, R. J. Nicholas, P. Pfeffer, W. Zawadzki, D. Gauthier, J. C. Portal, and M. A. DiForte-Poisson, Semicond. Sci. Technol. **2**, 568 (1987).
- [45] I. Gorczyca, P. Pfeffer, and W. Zawadzki, Semicond. Sci. Technol. **6**, 963 (1991).
- [46] B. K. Meyer, A. Hofstaetter, U. Leib, D.M. Hofmann J. Crys. Growth **184-185**, 1118 (1998).
- [47] D. Sprinzl, P. Horodyska, N. Tesarova, E. Rozkotova, E. Belas, R. Grill, P. Maly, and P. Nemeec, ArXiv 1001.0869.
- [48] C. Weisbuch and C. Hermann, Solid State Commun. **16**, 659 (1975).
- [49] M. Kubisa, K. Ryczko, and J. Misiewicz, Phys. Rev. B **83**, 195324 (2011).
- [50] A. A. Kiselev, E. L. Ivchenko, and U. Roessler, Phys. Rev. B **58**, 16353 (1998).
- [51] I. A. Yugova, A. Greilich, D. R. Yakovlev, A. A. Kiselev, M. Bayer, V. V. Petrov, Yu. K. Dolgikh, D. Reuter, and A. D. Wieck, Phys. Rev. B **75**, 245302 (2007)
- [52] K. L. Litvinenko, L. Nikzad, C. R. Pidgeon, J. Allam, L. F. Cohen, T. Ashley, M. Emeny, W. Zawadzki, and B. N. Murdin, Phys. Rev. B **77**, 033204 (2008).
- [53] W. Zawadzki, in *Narrow Gap Semiconductors, Physics and Applications*, edited by W. Zawadzki, (Springer, Berlin, 1980), p. 85.
- [54] P. Pfeffer and W. Zawadzki, Phys. Rev. B **74**, 233303 (2006).